

Frequency Domain Electromagnetic Soundings of Canadian Deep Permafrost

Kimmo Korhonen, Timo Ruskeeniemi, Markku Paananen and Jukka Lehtimäki

Geological Survey of Finland, P.O. Box 96, FI-02151 Espoo, Finland

(Received: April 2009; Accepted: September 2009)

Abstract

Frequency domain electromagnetic soundings were carried out at the Lupin gold mine and Ulu gold prospect in Northern Canada by the Geological Survey of Finland to investigate the lateral and vertical conditions of deep permafrost. The results indicate a deep seated electrical conductor in approximately half of the soundings. The detected conductor is interpreted as unfrozen and porous rock underneath the permafrost base saturated with saline groundwater. The mean depth of the permafrost base is 589 m and 476 m at the Lupin mine and Ulu prospect, respectively. The permafrost base, as deep as few hundreds of meters, can be detected using frequency domain electromagnetic soundings.

Key words: frequency domain electromagnetic soundings, permafrost, Canada

1. Introduction

Perennially frozen ground or permafrost is widespread at high latitudes and altitudes (e.g., *Yershov*, 1991; *Heginbottom et al.*, 1995; *Brown et al.*, 1998). It has a strong impact on landscapes, ecosystems and man-made infrastructures. Thus, the climate warming in the permafrost areas has created a concern about the degradation of permafrost. The impacts of this degradation include the thickening of the active layer and the consequent instability of the land surface and in longer term the changes in flora and fauna (*Harris*, 2005). Failing ground under buildings and oil and gas pipelines are widely reported from Russia and North America. Even more concerning is the potential release of methane from the melting soil (*Walter et al.*, 2006; *Mastepanov et al.*, 2008).

A large number of monitoring stations have been established all over the world to measure the changes in surface ground temperatures (CALM; <http://www.udel.edu/Geography/calm/>). Temperature profiling has also been conducted in numerous deep boreholes to assess the rate and impacts of the warming. Furthermore, there is a strong demand to obtain information covering larger areas and deeper regimes. Thus, various geophysical methods have been tested for this purpose.

A wide range of geophysical methods have been used in mapping the distribution of permafrost laterally and vertically (e.g., see the review by *Scott et al.*, 1990). The

direct-current resistivity methods (e.g. *Osterkamp et al.*, 1980; *Osterkamp and Jurick*, 1981; *King et al.*, 1987; *Hauck et al.*, 2000), ground and airborne electromagnetic methods (e.g. *Hoekstra*, 1978; *Kellett et al.*, 2000; *Hauck et al.*, 2000) and seismic methods (e.g. *Morack and Rogers* 1981; *Wagner*, 1996) are widely used. The applicability of geophysical methods to permafrost investigations is based on the cryogenic contrast in the relevant physical parameters between the frozen and unfrozen ground (e.g., *Scott et al.*, 1990).

The above geophysical investigations are mainly concerned with the mapping of shallow permafrost. In this paper we describe the application of a frequency-domain electromagnetic method (*Soininen and Jokinen*, 1991) for investigating the thickness of deep permafrost in resistive crystalline bedrock environment at the Lupin gold mine and Ulu gold prospect in Northern Canada.

The motivation behind these investigations has been the evaluation of the performance of the final disposal concept for spent nuclear fuel. Some climate models (*Imbrie and Imbrie*, 1980; *Loutre and Berger*, 2000) and simulations (*King-Clayton et al.*, 1995, *Kjellström et al.*, 2009) predict a large range of possible climates for the Northern and Central Europe and Northern America on a 100 000 year time perspective. This is the time period that needs to be included in analyses of long-term safety of repositories for spent nuclear fuel. Since the scenarios include also permafrost conditions, it has become essential to be able to assess the kinds of conditions that could form in the repository itself and in its surrounding environment in the future. To evaluate the performance of the repository, some kind of quantification of the possible hydrogeochemical and hydrogeological effects of permafrost is required. The jointly funded international Permafrost Project was established for this purpose. The project includes participants from Finland (the Geological Survey of Finland and Posiva), Sweden (Svensk Kärnbränslehantering; SKB), Great Britain (Nirex Ltd.) and Canada (Ontario Power Generation and the University of Waterloo).

2. Study sites

The Lupin gold mine and Ulu gold prospect are located in the Nunavut Territory, Canada, in the zone of continuous permafrost (Fig. 1). They are remote locations relying on air transportation most of the year. The mean surface air temperature at both sites is approximately $-10\text{ }^{\circ}\text{C}$ with minimum and maximum recorded temperatures of ca. -50 and $+30\text{ }^{\circ}\text{C}$, respectively. Furthermore, the climate is arid with low annual precipitation; the mean annual precipitation at the Lupin mine was 270 mm over the period 1983–2001 (*Ruskeeniemi et al.*, 2002).

The study sites are located in the Canadian Shield in an Archean metaturbidite sequence which has been tectonically stable for ca. 2.5 Ga with the exception of some Proterozoic faulting and intrusive activity (*Bullis et al.*, 1994; *Geusebroek and Duke*, 2004; *Ruskeeniemi et al.*, 2002; *Kleespies*, 1994). Both sites share the same geological feature of partly metamorphosed and partly preserved sedimentary rocks. The lithology of the Lupin mine is characterised by quartz feldspar gneiss and phyllite (*Bullis et al.*,

1994; Geusebroek and Duke, 2004; Ruskeeniemi *et al.*, 2002) whereas the lithology at the Ulu prospect is more complex. The central part of the Ulu prospect features a fold structure with alternating layers of fine-grained basalts, coarser grained gabbroic intrusions and metasediments (Kleespies, 1994).

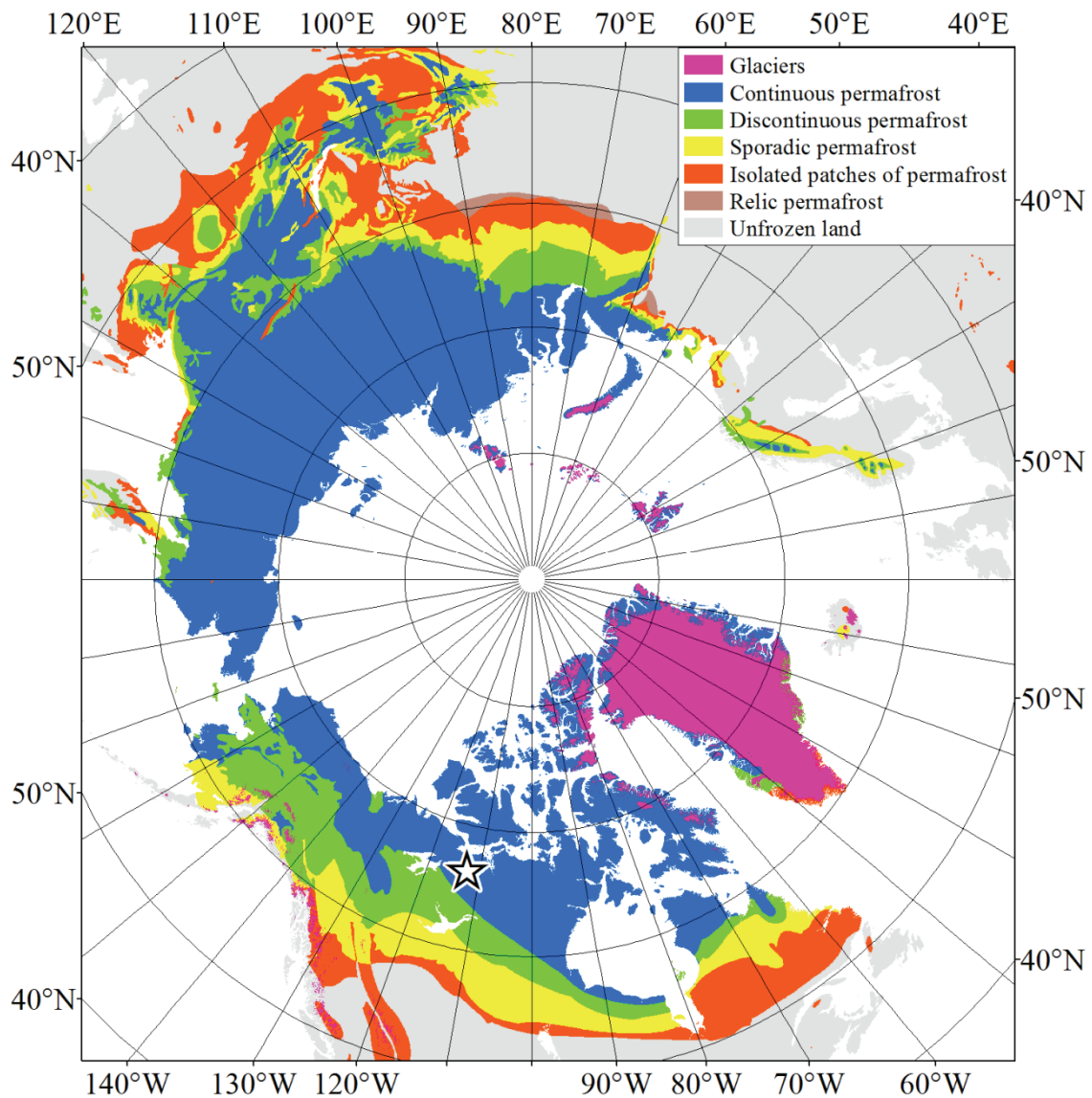


Fig. 1. The occurrence of permafrost in the northern hemisphere (Brown *et al.*, 1998). The Lupin mine and Ulu prospect (indicated with the star symbol) are located in the zone of continuous permafrost in the Nunavut Territory, Canada.

3. Permafrost

In areas where the mean annual air temperature remains below $-3\text{ }^{\circ}\text{C}$, such as the Lupin mine and Ulu prospect, the mean annual ground temperature drops below $0\text{ }^{\circ}\text{C}$ for at least two consecutive years and the freezing front descends deep enough to keep the ground frozen throughout the year. Such perennially frozen ground is termed permafrost and has the three-layer structure shown in Fig. 2a: (1) the active layer on top

freezes and thaws according to air temperature variations, (2) the permafrost layer in the middle remains below 0 °C throughout the year, and (3) the unfrozen ground underneath the permafrost base. In intact crystalline bedrock, there is little or no water to freeze and permafrost is defined simply as rock that remains below 0 °C. The temperature profile at the Lupin mine gives a good example of frozen ground temperatures in crystalline bedrock under deep permafrost conditions (Fig. 2b).

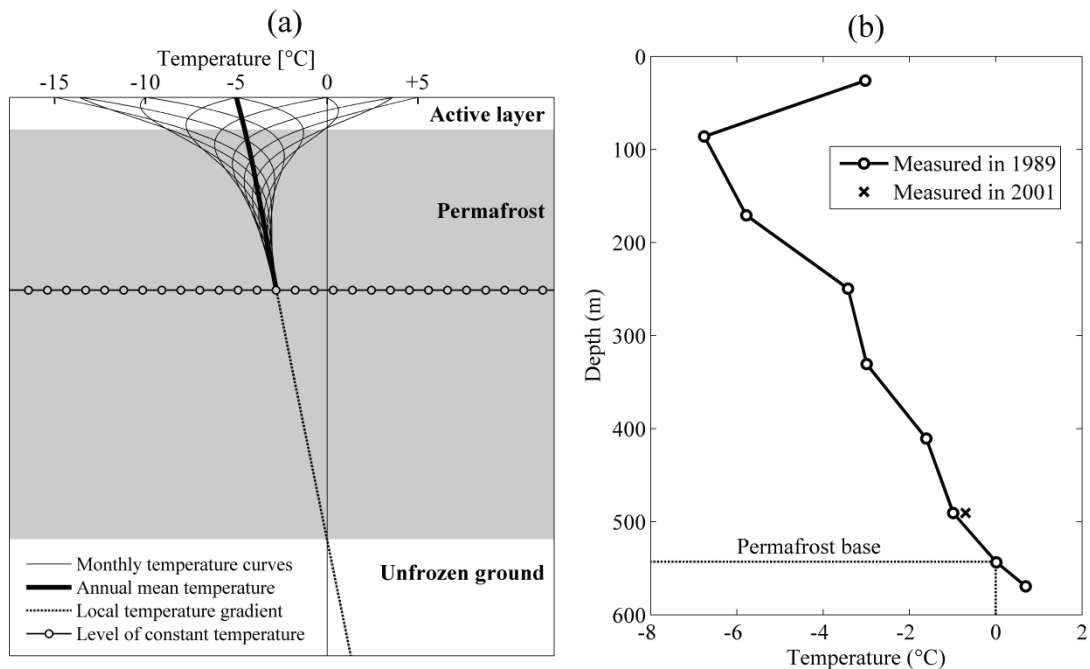


Fig. 2. Temperature profiles in permafrost ground. (a) A schematic illustration of the layered structure of permafrost showing the annual ground temperature variations due to surface temperature variations (mean surface temperature of -5 °C with a minimum of -15 °C in January and a maximum of +5 °C in July) and the local temperature gradient due to the geothermal heat-flux coming from the Earth's core. (b) Observations of ground temperatures at the Lupin mine (mean annual air temperature of -10 °C) indicating the permafrost base at a depth of about 540 m (Sandhu and Tansey, 1996; Ruskeeniemi et al., 2002). Note the uppermost ground temperature affected by the mining activities. The true temperature at the depth of 25 m is about -7 °C according to the bedrock surface temperatures observed by thermistors installed through the soil cover (an unpublished report by the Echo Bay Mines Ltd).

Perennially frozen ground conditions prevail in extensive land areas at high latitudes and high altitudes (Fig. 1). The depth of permafrost may exceed hundreds of meters and as such indicates the existence of long-term cold and arid climate for thousands of years. Permafrost has a strong impact, not only on the landscape and ecosystem, but also on the subsurface conditions, such as the groundwater flow and formation of methane clathrates at depth.

4. Frequency domain electromagnetic soundings

A wide-band frequency-domain electromagnetic (EM) sounding system called Sampo was used to carry out the soundings at the Lupin mine and Ulu prospect. The system was designed and constructed by Outokumpu Electronics in co-operation with

the Geological Survey of Finland in the late 1980s (*Soininen and Jokinen, 1991*). The system consists of a horizontal transmitter loop and a receiver of three perpendicular coils (Fig. 3). The transmitter loop is used to generate a magnetic primary field at 82 discrete frequencies between 2 Hz and 20 kHz. The primary field induces secondary magnetic fields in subsurface conductors. The receiver coils are used to measure the radial, tangential and vertical components (X , Y and Z , respectively) of the superposition of the primary and secondary magnetic fields (the total magnetic field) at a distance from the transmitter.

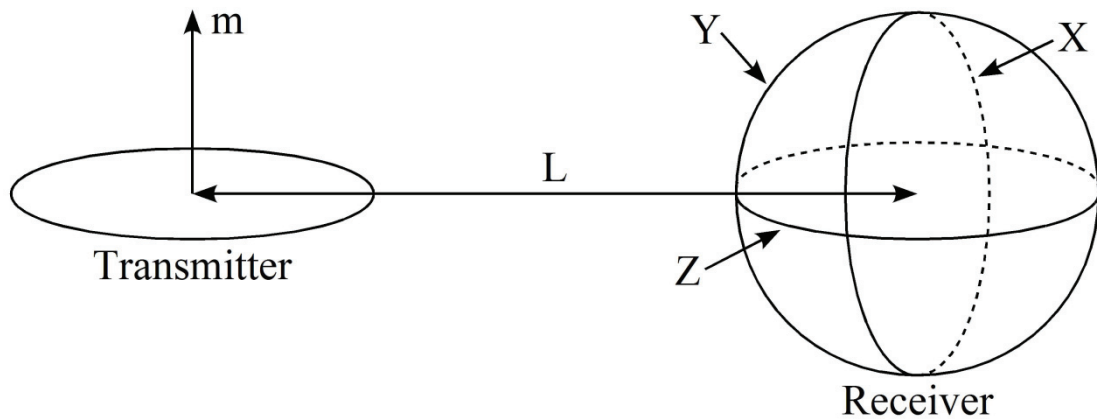


Fig. 3. A schematic illustration of the frequency domain electromagnetic sounding system. The transmitter is a horizontal wire loop which is equivalent to a vertical magnetic dipole of the moment m . The receiver consists of three perpendicular coils measuring the radial, tangential and vertical components (X , Y and Z , respectively) of the magnetic field at the distance L from the transmitter.

The skin depth is a measure of the attenuation of electromagnetic fields due to the medium in which they travel. It is defined as

$$\delta = \sqrt{\frac{2}{\sigma \cdot \mu \cdot \omega}} \quad (1)$$

where σ and μ are the electrical conductivity and magnetic permeability of the medium, and ω is the angular frequency of the field (*Peltoniemi, 1988*). The skin depth indicates the distance after which the field has lost 63% of its energy. Because the skin depth depends inversely on the frequency of the field, fields of lower frequencies penetrate deeper into the ground than those of higher frequencies. Assuming the ground to be horizontally layered, it is the vertical-to-radial component ratios $R_i = Z_i/X_i$ at each frequency f_i that convey information about the vertical conductivity structure of the subsurface from different depths roughly at the midpoint between the transmitter and receiver.

For qualitative interpretation, the ratios R_i (Fig. 4a) are transformed into curves of apparent resistivity as a function of depth (ARD curves; Fig. 4b) using the algorithm of *Aittoniemi et al. (1987)*. Quantitative interpretation of the soundings is performed using

a computer program (Sipola, 2002) that fits the response from a 1-D layered-earth model to the observed ratios R_i (Fig. 4b) using non-linear optimization.

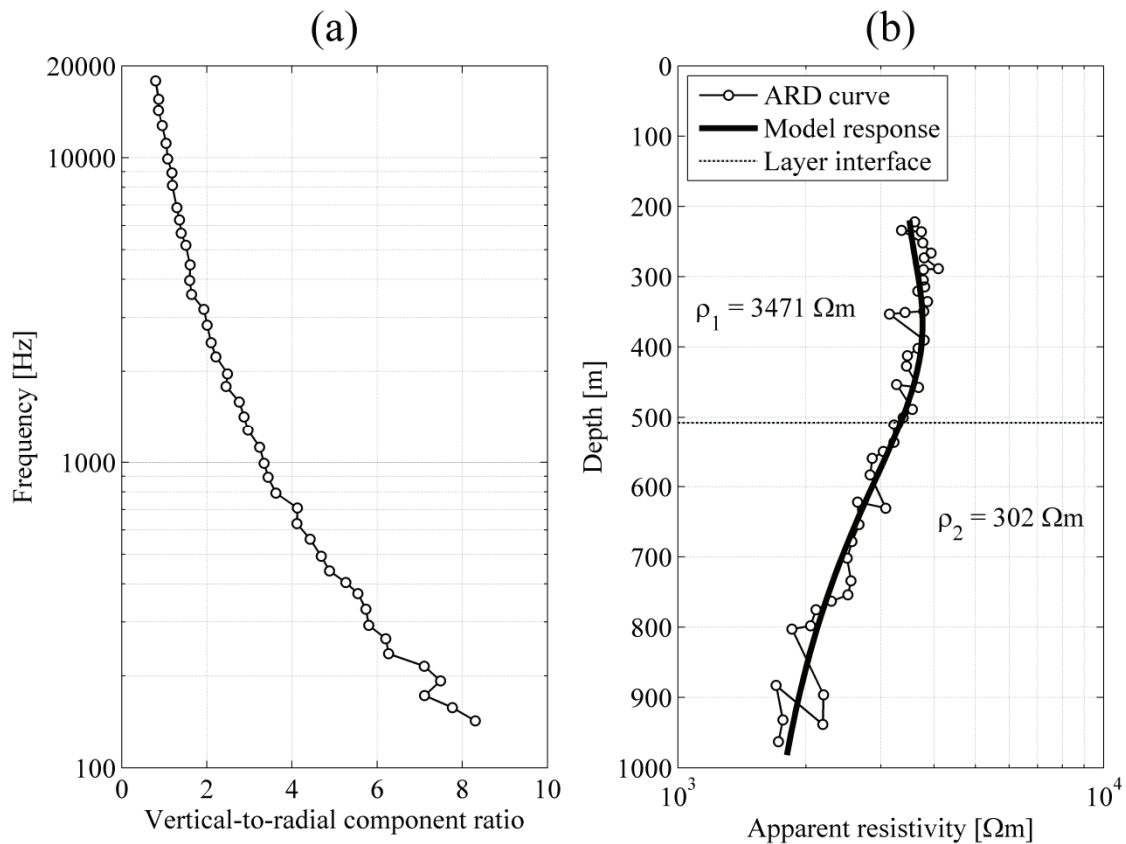


Fig. 4. Results from an EM sounding at the Ulu prospect. (a) The vertical-to-radial component ratios for the sounding. (b) The observed ratios in (a) transformed into a curve of apparent resistivity as a function of depth (ARD curve) for qualitative interpretation. The quantitative interpretation was obtained by fitting a two-layer model (ρ_1 and ρ_2 are the resistivities of the model layers) to the observed ratios in (a).

The EM soundings are typically carried out at regularly spaced measurement stations along straight measurement lines keeping the transmitter-receiver distance (the coil separation) fixed. The coil separation is chosen according to the desired depth of investigation. Larger coil separations are used for higher depths of investigation and require larger loops with higher magnetic moments. Typical coil separations are within the range of 50 to 1500 meters. Transmitter loops of 10, 20 and 65 m diameter are available for the soundings.

The depth of investigation of the EM system depends not only on the frequencies employed and the electrical properties of the ground but also on the coil separation used. In resistive environments, the depth of investigation can be several kilometers. However, during interpretation, information coming below the depth equal to one or two coil separations is considered unreliable.

5. *Sensitivity of the EM system to a deep conductive layer underneath a resistive layer*

Electrical conductivity is the relevant physical parameter that the EM soundings respond to. Even intact crystalline rocks contain some amount of porosity which is often filled with more or less saline groundwater. The occurrence of saline groundwater increases the electrical conductivity (or conversely, decreases the electrical resistivity) of crystalline rocks. When bedrock temperatures drop below 0 °C, the groundwater contained in the pores begins to freeze, decreasing the electrical conductivity of the frozen crystalline rock as the freezing immobilizes the free charge carriers present in saline groundwater. This creates a cryogenic conductivity contrast between the frozen and unfrozen rocks underneath the permafrost base.

It should be noted that salinity (the amount of dissolved solids) lowers the freezing point of water. For example, ocean water with the salinity of 35 g/l freezes at -2 °C. *Gilichinsky et al.* (2003) report brines (with salinities in the range of 170–300 g/l) from Siberian marine sediments which remain liquid even at -10 °C. However, this is a rare circumstance which is not relevant in low-porosity crystalline rocks.

To test the ability of the EM system to detect a deep seated cryogenic conductivity contrast, a two-layer model was used. The top layer is the frozen bedrock with resistivity values of 5, 10 and 20 kΩm typically encountered in dry crystalline rocks without saline pore water. The bottom layer is the unfrozen rock. The roof of the unfrozen rock layer is located at the depth of 500 m. The resistivity of the saturated unfrozen rock is calculated from a small-sphere porosity model (*Grant and West, 1965*) as

$$\rho_2 = \frac{2 \cdot \rho_1 + \rho_w + (n - 1) \cdot (\rho_w - \rho_1)}{2 \cdot \rho_1 + \rho_w + 2 \cdot (1 - n) \cdot (\rho_w - \rho_1)} \cdot \rho_w \quad (2)$$

where ρ_1 is the resistivity of the frozen rock layer, ρ_2 is the resistivity of the saturated unfrozen rock layer, ρ_w is the resistivity of the saline pore water, and n is the porosity of the rock. A critical value ρ_c for the groundwater resistivity ρ_w was assessed to have a response from a two-layer model that is significantly different from the response of a homogenous half-space of resistivity ρ_1 .

95% confidence intervals were estimated for the ARD curves of the two-layer models to determine significant difference from the half-space model. The estimation was performed using Monte Carlo simulations. The X and Z components of each two-layer model response were first calculated and white noise was added to the components. The noise is 2% for high frequencies and increases exponentially to 20% for the low frequencies. This is a valid assumption because the sampling procedure used by the EM system is typically set to produce results having a 2% maximum error with a confidence level of 68%. At higher frequencies the procedure usually converges well but at lower frequencies it diverges and results get progressively noisier. The vertical-to-radial component ratios R_i were then calculated for each frequency f_i using the noise-

perturbed components. This was repeated 10 000 times, and the 2.5 and 97.5 percentiles of R_i were taken as the lower and upper 95% confidence intervals. The confidence intervals were then transformed into ARD curves.

Two cases were tested with the porosity values of 0.3 and 0.5% (Fig. 5). These values are typical for intact crystalline rocks (e.g., *Gehör et al.*, 2007). The results of the tests (Fig. 5) indicate that even weakly saline groundwater causes a cryogenic conductivity contrast at a depth of 500 m detectable using a coil separation of 800 m. According to an investigation carried out at the Lupin mine (*Ruskeeniemi et al.*, 2002; *Ruskeeniemi et al.*, 2004; *Stotler et al.*, 2009), the electrical conductivity of groundwater in the unfrozen rock varies somewhere between 200 and 600 mS/m (5 and 2 Ωm). Thus, even with low porosity (0.3%) and resistivity (5 $\text{k}\Omega\text{m}$) conditions, the EM system should be able to detect the cryogenic conductivity contrast. For instance, the critical resistivity value of $\rho_c = 14 \Omega\text{m}$ corresponds to groundwater conductivity of 71 mS/m which is well below the lower-end value of 200 mS/m measured at this site.

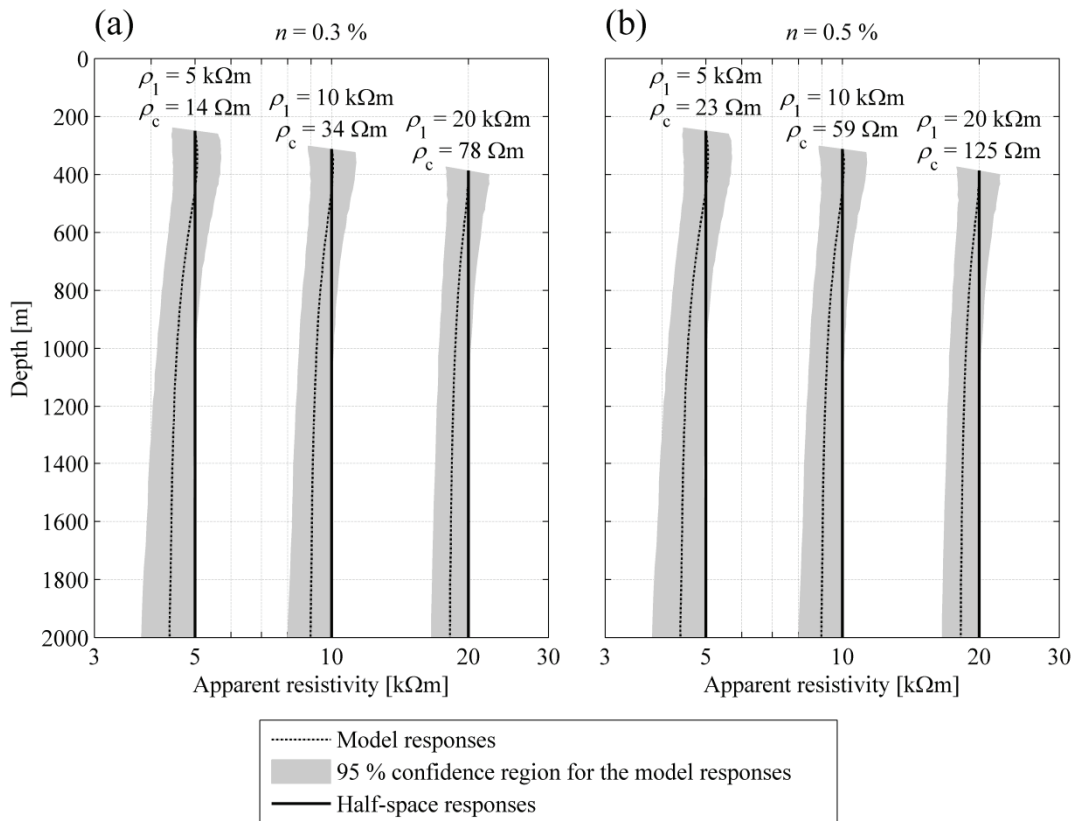


Fig. 5. Testing the sensitivity of the EM system to a cryogenic conductivity contrast at the depth of 500 m using the coil separation of 800 m. Two typical values of porosity of (a) $n = 0.3\%$ and (b) $n = 0.5\%$ were used. Bedrock resistivity is ρ_1 and the critical groundwater resistivity required to produce a response that is significantly different from the half-space response is ρ_c . The broken lines show the ARD curves for the two-layer model responses, the shaded areas show the 95% confidence regions for the model responses, and the solid lines show the half-space model response. In (a) the ρ_1/ρ_2 contrasts required for detection are 80, 66 and 58 corresponding to the critical groundwater resistivity of 14, 34 and 78 Ωm ; and in (b) the ρ_1/ρ_2 contrasts are 49, 39 and 36 corresponding to the values of critical groundwater resistivity of 14, 34 and 78 Ωm .

6. Results of the investigations

In total, 129 EM soundings along 8 lines were carried out at the Lupin mine in June 2002 (Fig. 6a) to assess the depth to the permafrost base (Paananen and Ruskeeniemi, 2003). The EM soundings at the Ulu prospect were carried out in June 2005 (Fig. 6b). The depth of the permafrost base was probed along 10 lines containing 116 soundings.

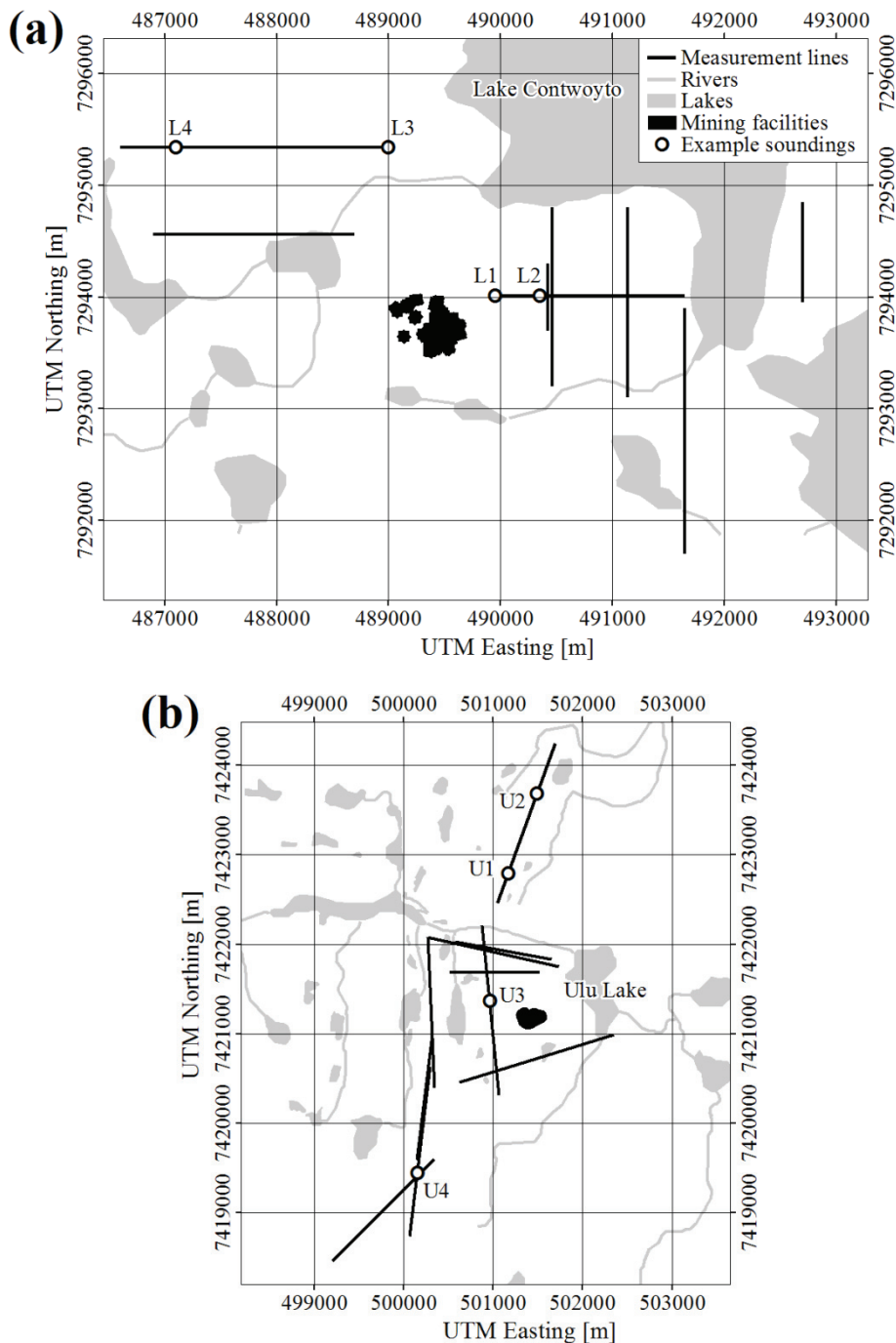


Fig. 6. Locations of the EM measurement lines at the (a) Lupin mine and (b) Ulu prospect. The circles indicate the locations of the example soundings shown in Figs. 7 and 8.

The soundings were interpreted according to 1-D layered-earth models of two or three layers (e.g. *Paananen and Ruskeeniemi, 2003*). The top layer is the permafrost with a considerably higher resistivity than the bottom layer representing the unfrozen bedrock saturated by saline pore water. In some cases, additional low-resistivity layers were needed to account for the influence of a conductive overburden or mineral formation. A deep electrical conductor was identified in 57% of all soundings at the Lupin mine. For the Ulu prospect, this percentage is somewhat lower; 45% of all soundings indicate a deep electrical conductor. About half of all soundings could be interpreted using a 1-D layered earth model. The rest of the soundings were either too noisy, or effects from 3-D geometries violated the 1-D layered earth assumption.

Figs 7 and 8 show examples of EM soundings carried out at the Lupin mine (the soundings L1–L4) and Ulu prospect (the soundings U1–U4). The interpretations of the soundings L1 and L2 indicate the permafrost base at a depth of about 520 meters, corresponding well with the depth of about 540 m estimated from observations (Fig. 2b). A three-layer model with a conductive overburden was required to achieve a good fit to the sounding L1 whereas a two-layer model was sufficient in the case of the sounding L2. The EM method is sensitive to conductivity contrasts and can resolve the location of a good conductor accurately. However, the method cannot resolve the high resistivity of the permafrost accurately, which explains the large difference in the resistivity of the permafrost between the soundings L1 and L2. The interpretations of the soundings U1 and U2 also show clear indications of the permafrost base even though these interpretations display much larger variation in the depth and resistivity of the conductive layer underneath the permafrost. The sounding L3 provides an example of a sounding that gives no indication of a deep electrically conductive layer; it merely indicates a resistive homogenous half-space. The sounding L4 is contaminated with EM noise and was not interpreted. The soundings U3 and U4 illustrate typical characteristics of soundings carried out near geological formations or human constructs that violate the 1-D layered-earth assumption and were not interpreted.

To estimate the spatial distributions of the depth of the permafrost base and the resistivity of the electrically conductive layer underneath the permafrost, the successfully interpreted depths of the roof of the deep conductive layer and its resistivities were interpolated to a regular grid using the inverse distance weighting method (*Davis, 2002*). The depth or resistivity at a grid point was calculated using

$$f(x, y) = \frac{\sum_{i=1}^N w_i^p \cdot z_i}{\sum_{i=1}^N w_i^p} \quad (3)$$

where $f(x, y)$ is the interpolated value at a grid point, N is the number of observations within a search radius, w_i is the inverse of the Euclidean distance between the i th observation at (x_i, y_i) and the grid point, z_i is the value of the i th observation, and p is the inverse distance power.

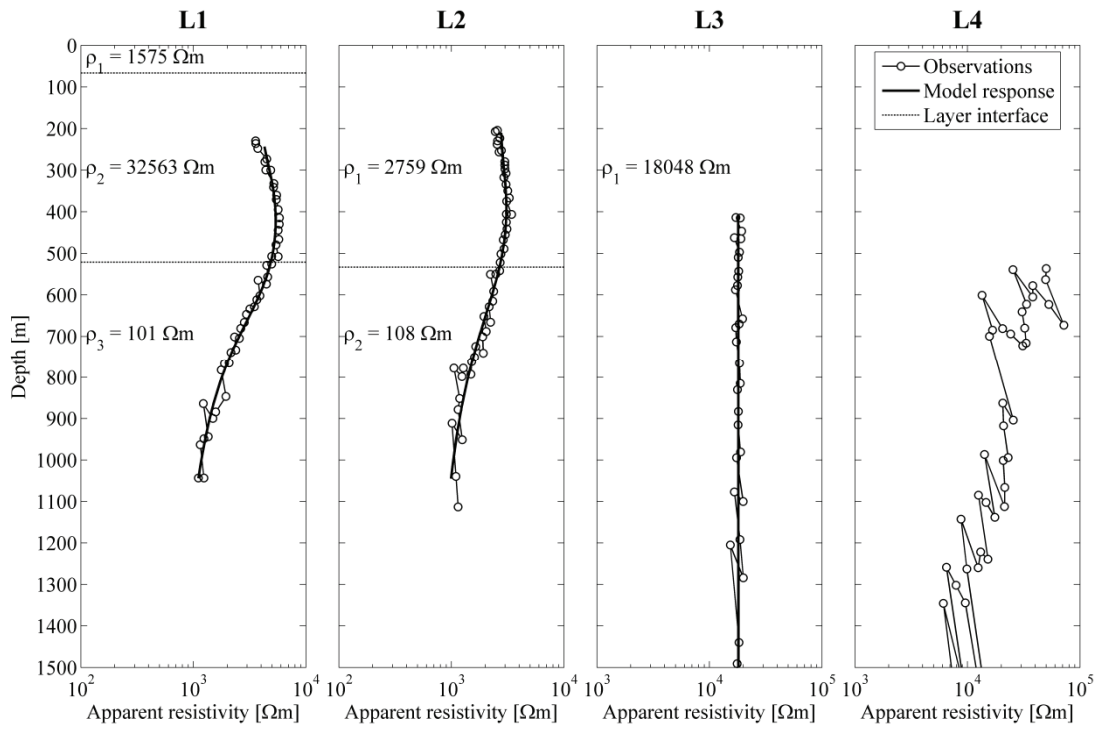


Fig. 7. Examples of EM soundings from the Lupin mine. The soundings L1 and L2 were interpreted with a three-layer and two-layer model, respectively, and show a clear indication of the permafrost base at about 520 m. The sounding L3 merely indicates a resistive half space. The sounding L4 is contaminated with EM noise. The locations of the soundings L1–L4 are shown in Fig. 6a.

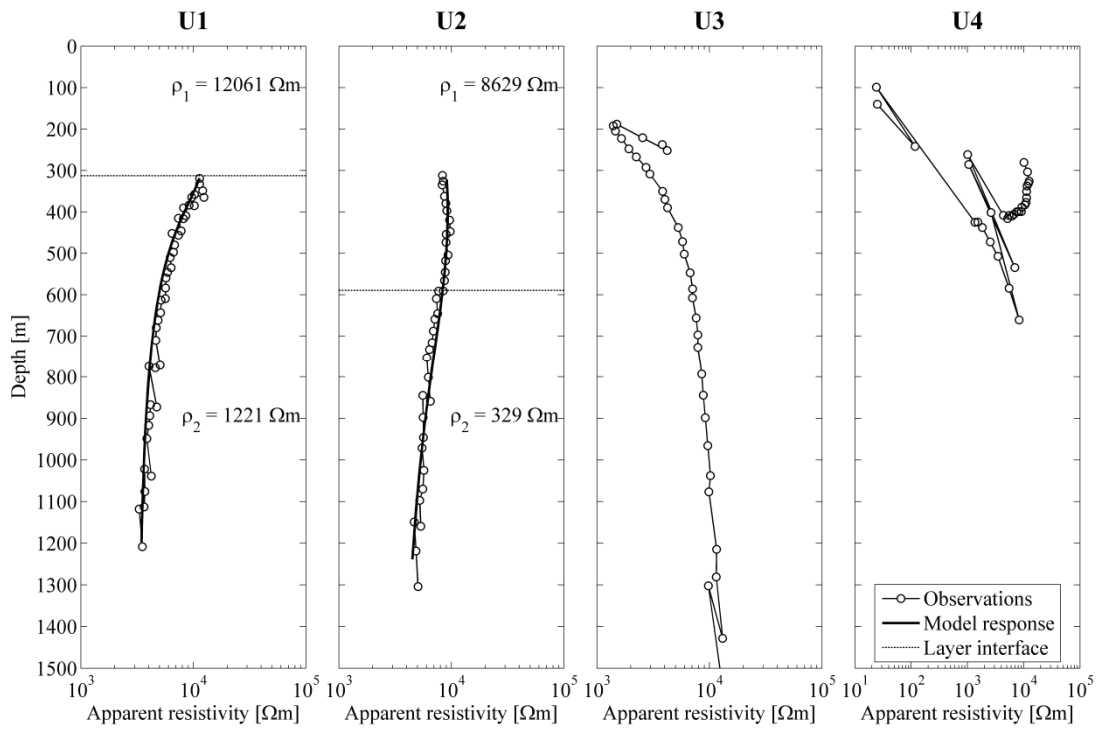


Fig. 8. Examples of EM soundings from the Ulu prospect. The soundings U1 and U2 were interpreted with two-layer models and show clear indications of the permafrost base at about 300 and 600 m respectively. The soundings U3 and U4 were carried out near geological formations or human constructs that violate the 1-D layered-earth assumption. The locations of the soundings U1–U4 are shown in Fig. 6b.

There is scatter in the interpreted conductor depths and resistivities even in some near-by soundings. For instance, the interpretations of the soundings U1 and U2 which are located 950 m apart indicate a 300 m difference in the depth of the permafrost base and nearly a fourfold difference in the resistivity of the deep conductor. The mean interpreted conductor depth and resistivity for the Lupin mine is 589 m and 330 Ωm , respectively; the standard deviation of the conductor depth is 114 m and most of the interpreted resistivities are within the range of 134–815 Ωm . For the Ulu prospect the mean conductor depth and resistivity is 476 m and 812 Ωm , respectively; the standard deviation of the conductor depth is 173 m and most of the interpreted resistivities are within the range of 372–1775 Ωm . To smooth the scatter, an inverse distance power of 0.5 and search radius of 1 km were used to produce the spatial distributions of the depth of the permafrost base (Fig. 9) and the resistivity of the conductive layer underneath the permafrost (Fig. 10).

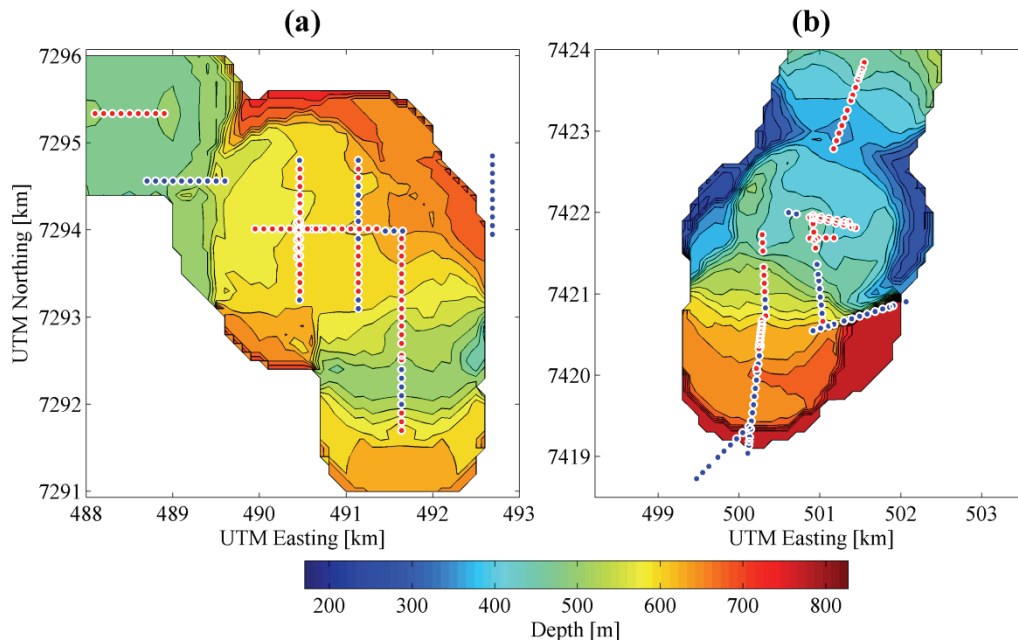


Fig. 9. The estimated depths to the permafrost base for the (a) Lupin mine and (b) Ulu prospect. The red symbols indicate soundings for which a deep seated electrical conductor was successfully interpreted whereas the blue symbols indicate soundings with no indication of a deep electrical conductor.

7. Discussion and conclusions

Numerical modelling indicates that the EM system can detect a deep seated cryogenic conductivity contrast even in low-porosity crystalline rocks saturated with weakly saline groundwater. Approximately half of the soundings carried out at the Lupin mine and Ulu prospect show a clear indication of a contrast. The mean depth of the permafrost base at the Lupin mine is 589 m corresponding well with the depth estimate from the temperature profile (Fig. 2b). For the Ulu prospect, no temperature profile is available to assess the depth of the permafrost base. However, the mean depth of the permafrost base of 476 m seems plausible considering the similarities between the two study sites.

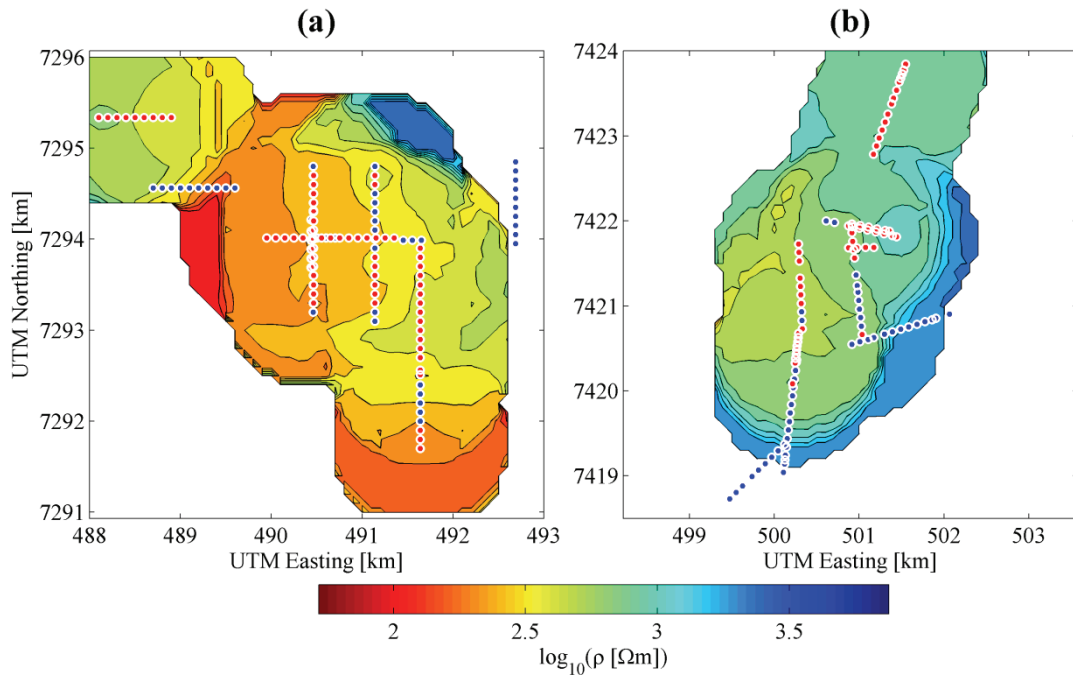


Fig. 10. The estimated resistivities of the electrical conductor underneath the permafrost base for the (a) Lupin mine and (b) Ulu prospect. The red and blue symbols are as in Fig. 9.

Hydrogeochemical studies at the Lupin mine indicate that the growth of deep permafrost is not able to generate a supersaline out-freezing front (fractionation of dissolved solids between ice and water) in low-porosity crystalline bedrock (*Zhang and Frapce, 2003; Ruskeenieni et al., 2004; Stotler et al., 2009*). However, the groundwater underneath the permafrost base is brackish with observed conductivities ranging from 500 to 700 mS/m. Such conditions are well detectable by the EM system according to the numerical modeling (Fig. 5) and the results of the EM soundings (Figs 7 and 8).

The results from the Ulu prospect show considerable scatter whereas the variations in the results from the Lupin mine are smaller (Fig. 9). The depth of the permafrost base also appears to have a northeast trend at both sites. Spatial variation in porosity, groundwater salinity and lithology are likely causes for the scatter in the results. Particularly, the lithology at the Ulu prospect is complex with a fold structure of alternating rocks dominating the geology of the central part of the surveyed area. Furthermore, surface and underground mining activities and infrastructures most likely cause active and passive EM noise (*Szarka, 1988*) which is likely to make it more difficult to detect saline groundwater in depth. In addition, there are some unavoidable sources of errors due to surveying conditions; the incorrect orientation of the receiver and topographical effects (the transmitter and receiver are not on the same horizontal plane). However, these errors can be corrected and should not affect the results too much.

There is not much direct evidence concerning the lateral depth variations of permafrost. Even the localized temperature data is generally coming from few scattered thermistors in boreholes or in mine workings. However, there is some unpublished data from Canadian mines showing that massive ore units are frozen deeper than the

surrounding barren wall rocks. It is not well understood how much the base of deep permafrost (> 200 m) can fluctuate due to surficial factors, e.g., vegetation, snow thickness and soil type. Thus, the observed variations in the depth of the permafrost base are in a range which may be explained by natural and anthropogenic factors.

The resistivities of the deep conductors (Fig. 10) also show large scatter. However, this scatter is quite expected since the method cannot resolve the resistivities as accurately as depths. Also, it is typical that electrical resistivity varies in a wide range even within a single rock unit because even small variations in the amount and salinity of groundwater can cause considerable changes in the bulk resistivity of rocks. Thus, the scatter in the resistivities should be adequately explained by spatial variations in porosity, groundwater salinity and lithology.

Acknowledgements

We thank Ilkka Suppala and Seppo Elo of the Geological Survey of Finland for helpful comments. We also thank Dr. Richard Fortier of Université Laval for comments that helped to improve this paper.

References

- Aittoniemi, K., J. Rajala and J. Sarvas, 1987. Interactive Inversion Algorithm and Apparent Resistivity Versus Depth (ARD) Plot in Multifrequency Depth Soundings. *Acta Polytechnica Scandinavica Applied Physics Series*, **157**, 34 pp.
- Brown, J., O.J. Ferrians, Jr., J.A. Heginbottom and E.S. Melnikov, 1998. Circum-Arctic map of permafrost and ground-ice conditions. Revised February 2001, World Data Center for Glaciology, National Snow and Ice Data Center, Boulder, Colorado. Digital media.
- Bullis, H.R., R.A. Hureau and B.D. Penner, 1994. Distribution of gold and sulphides at Lupin, Northwest Territories. *Economic Geology*, **89**, 1217–1227.
- CALM. The Circumpolar Active Layer Monitoring Network—CALM II (2004-2008): Long-Term Observations of the Climate–Active Layer–Permafrost System. URL: <http://www.udel.edu/Geography/calm/>. Accessed Sep 1 2009.
- Davis, J.C., 2002. Statistics and data analysis in geology. John Wiley & Sons, New York, 656 pp.
- Gehör, S., A. Kärki and M. Paananen, 2007. Petrology, Petrophysics and Fracture Mineralogy of the Drill Core Sample OL-KR19 and OL-KR19B. Posiva Oy, Working Report 2007-44, 51 pp.
- Geusebroek, P.A. and N.A. Duke, 2004. An Update on the Geology of the Lupin Gold Mine, Nunavut, Canada. *Exploration and Mining Geology*, **13**, 1–13.
- Gilichinsky, D., E. Rivkina, V. Shcherbakova, K. Laurinavichuis and J. Tiedje, 2003. Supercooled Water Brines Within Permafrost – An Unknown Ecological Niche for Microorganisms: A Model for Astrobiology. *Astrobiology*, **3**, 331–341.

- Grant, W. and G. West, 1965. Interpretation theory in applied geophysics. McGraw-Hill, New York, 583 pp.
- Harris, C., 2005. Climate change, mountain permafrost degradation and geotechnical hazard. In: Huber, U.M., H.K.M. Bugmann and M.A. Reasoner (eds.), 2005. Global Change and Mountain Regions: An Overview of Current Knowledge, *Advances in Global Research*, **23**, 215–224.
- Hauck, C., D. Vonder Mühl, N. Russill and K. Isaksen, 2000. An integrated geophysical study to map mountain permafrost: A case study from Norway. Proceedings of the 6th EEGS conference, 3–6 September 2000, Bochum, Germany, Extended Abstracts, CH01.
- Heginbottom, J.A., M.A. Dubreuil and P.A. Harker (compilers), 1995. Canada – Permafrost. In: National Atlas of Canada, 5th Edition, National Atlas Information Service, National Resources Canada, MCR 4177.
- Hoekstra, P., 1978. Electromagnetic methods for mapping shallow permafrost. *Geophysics*, **43**, 782–787.
- Imbrie, J. and J.Z. Imbrie, 1980. Modelling the climatic response to orbital variations. *Science*, **207**, 943–953.
- Kellet, R., A. Hinnel, J. Gamey and G. Hodges, 2000. Mapping discontinuous permafrost in the Canadian Sub-Arctic using a combination of airborne and surface geophysical surveys. SEG annual convention, Extended Abstracts.
- King, L., W. Fisch, W. Haeberli and H.P. Wächter, 1987. Comparison of resistivity and radio-echo soundings on rock glacier permafrost. *Zeitschrift für Gletscherkunde und Glazialgeologie*, **23**, 77–97.
- King-Clayton, L.M., N.A. Chapman, F. Kautsky, N.-O. Svensson, G. de Marsily, and E. Ledoux, 1995. The central scenario for SITE-94: A climate change scenario. SKI Report 95:42, Swedish Nuclear Power Inspectorate, Stockholm.
- Kjellström, E., G. Strandberg, J. Brandefelt, J.-O. Näslund, B. Smith and B. Wohlfarth, 2009. Climate conditions in Sweden in a 100,000-year time perspective. Report SKB TR-09-04, Svensk Kärnbränslehantering AB, Stockholm.
- Kleespies, P.A. 1994. The geology and geochemistry of gold mineralization, Ulu claims, Northwest Territories, Canada. Master's thesis, University of Alberta, 217 pp.
- Loutre, M.F. and A. Berger, 2000. Future climate changes: Are we entering an exceptionally long interglacial? *Climatic Change*, **46**, 61–90.
- Mastepanov, M., C. Sigsgaard, E.J. Dlugokencky, S. Houweling, L. Ström, M.P. Tamstorf, and T.R. Christensen, 2008. Large tundra methane burst during onset of freezing. *Nature*, **456**, 628–630.
- Morack, J.L. and J.C. Rogers, 1981. Seismic evidence of shallow permafrost beneath the the Islands in the Beaufort Sea, Alaska. *Arctic*, **34**, 166–174.
- Osterkamp, T.E., R.W. Jurick, G.A. Gislason and S.I. Akasofu, 1980. Electrical resistivity measurements in permafrost terrain at the Engineer Creek road cut, Fairbanks, Alaska. *Cold Regions Science and Technology*, **3**, 277–286.

- Osterkamp, T.E. and R.W. Jurick, 1981. Detecting massive ground ice in permafrost by geophysical methods. *The Northern Engineer*, **12**, 27–30.
- Paananen, M. and T. Ruskeeniemi, 2003. Permafrost at Lupin: Interpretation of SAMPO electromagnetic soundings at Lupin. Geological Survey of Finland, Report YST-117, 28 pp.
- Peltoniemi, M., 1988. Maa- ja kallioperän geofysikaaliset tutkimusmenetelmät. Otakustantamo, Otaniemi, 411 pp. (In Finnish)
- Ruskeeniemi, T, L. Ahonen, M. Paananen, S. Frape, R. Stotler, M. Hobbs, J. Kaija, P. Degnan, R. Blomqvist, M. Jensen, K. Lehto, L. Morén, I. Puigdomenech and M. Snellman, 2004. Permafrost at Lupin: Report of Phase 2. Geological Survey of Finland, Report YST-119, 89 pp.
- Ruskeeniemi, T, M. Paananen, L. Ahonen, J. Kaija, A. Kuivamäki, S. Frape, L. Morén and P. Degnan, 2002. Permafrost at Lupin: Report of Phase 1. Geological Survey of Finland, Report YST-112, 59 pp.
- Sandhu, M. and C.M. Tansey, 1996. Echo Bay Mines Ltd. Lupin Mine Design. Internal report, 31 pp.
- Scott, W.J., P.V. Sellmann and J.A. Hunter, 1990. Geophysics in the study of permafrost. In: Ward, S.H. (ed.), 1990. Geotechnical and Environmental Geophysics, **Vol. 1**, Society of Exploration Geophysicists, Tulsa, Oklahoma.
- Sipola, V.-P., 2002. A new data processing and interpretation program for the Sampo electromagnetic multifrequency sounding system. Master's thesis, Helsinki University of Technology, Otaniemi, 69 pp.
- Soininen, H. and T. Jokinen, 1991. SAMPO, a new wide-band electromagnetic system. Technical Programme and Abstracts, EAEG 53rd Meeting and Technical Exhibition, Florence, Italy, 26–30 May, 1991, 366–367.
- Stotler, R.L., S.K. Frape, T. Ruskeeniemi, L. Ahonen, T.C. Onstott, and M.Y. Hobbs, 2009. Hydrogeochemistry of groundwaters in and below the base of thick permafrost at Lupin, Nunavut, Canada. *Journal of Hydrology*, **373**, 80–95.
- Szarka, L., 1988. Geophysical aspects of man-made electromagnetic noise in the Earth – a review. *Surveys in Geophysics*, **9**, 287–318.
- Wagner, S., 1996. DC resistivity and seismic refraction sounding on rock glacier permafrost in north-west Svalbard. *Norsk Geografisk Tidsskrift*, **50**, 25–36.
- Walter, K.M., S.A. Zimov, J.P. Chanton, D. Verbyla and F.S. Chapin, 2006. Methane bubbling from Siberian thaw lakes as a positive feedback to climate warming. *Nature*, **443**, 71–75.
- Yershov, E.D. (ed.) 1991. Geocryological map of Russia and neighbouring republics. Moscow State University, Russian Ministry of Geology. The English language edition, 1999. Collaborative Map Project, Carleton University, Ottawa, Canada.
- Zhang, M. and S.K. Frape, 2003. Evolution of shield brine groundwater composition during freezing. Ontario power Generation, Report No: 06819-REP-01200-10089-R00, 49 pp.